Neuron
Article

Comparison of Human Ventral Frontal Cortex Areas for Cognitive Control and Language with Areas in Monkey Frontal Cortex

Franz-Xaver Neubert,[1,*] Rogier B. Mars,[1,2] Adam G. Thomas,[2,3] Jerome Sallet,[1] and Matthew F.S. Rushworth[1,2]
[1]Department of Experimental Psychology, University of Oxford, 9 South Parks Road, Oxford OX1 3UD, UK
[2]Oxford Centre for Functional MRI of the Brain, Nuffield Department of Clinical Neurosciences, John Radcliffe Hospital, Headington, Oxford OX3 9DU, UK
[3]Functional MRI Facility, NIMH, National Institutes of Health, Bethesda, MD 20892-1148, USA
*Correspondence: franz-xaver.neubert@psy.ox.ac.uk
http://dx.doi.org/10.1016/j.neuron.2013.11.012

SUMMARY

Human ventrolateral frontal cortex (vlFC) is identified with cognitive processes such as language and cognitive flexibility. The relationship between it and the vlFC of other primates has therefore been the subject of particular speculation. We used a combination of structural and functional neuroimaging methods to identify key components of human vlFC. We compared how vlFC areas interacted with other brain areas in 25 humans and 25 macaques using the same methods. We identified a core set of 11 vlFC components that interacted in similar ways with similar distributed circuits in both species and, in addition, one distinctively human component in ventrolateral frontal pole. Fundamental differences in interactions with posterior auditory association areas in the two species were also present—these were ubiquitous throughout posterior human vlFC but channeled to different frontal regions in monkeys. Finally, there were some differences in interregional interactions within vlFC in the two species.

INTRODUCTION

The vlFC is identified with cognitive processes pre-eminent in humans such as language and cognitive flexibility. Broca's area is a part of left vlFC and is associated with language (Friederici and Gierhan, 2013), while other vlFC areas, sometimes in the right hemisphere, have been linked to cognitive control—high-level top-down control of behavior—by influencing processing in other brain regions (Aron, 2007; Brass et al., 2005; Dosenbach et al., 2006; Higo et al., 2011; Neubert et al., 2010).

Despite vlFC's identification with such aspects of human cognition, key features of its neuroanatomy, such as cytoarchitecture, seem homologous in human and nonhuman primates such as the macaque (Petrides and Pandya, 2002). Apparent homology in neuroanatomy is puzzling when macaques lack cognitive skills that humans possess. There is evidence that macaque vlFC is involved in auditory processing (Romanski, 2012), orofacial motor control (Petrides et al., 2005), and gesture recognition (Rizzolatti and Sinigaglia, 2010), which might relate to processes necessary for language. However, emphasis has also been placed on macaque vlFC's role in multimodal sensory integration (Passingham and Wise, 2012; Romanski, 2012), the selection of environmental features for attention, and their subsequent use to guide flexible decision making and action selection (Passingham and Wise, 2012). How the macaque brain areas responsible for these processes relate to areas in human vlFC areas implicated in attention and task control remains uncertain.

An alternative hypothesis is that there are new areas in human vlFC that support uniquely human cognitive abilities. A recent cytoarchitectonic and receptor-density-based investigation identified previously unreported vlFC regions in locations associated with language and cognitive control (Amunts et al., 2010). It is possible that no corresponding regions exist in monkeys but no test has been conducted. Alternatively, another aspect of vlFC may differ between species—the interactions that regions have with each other and with the rest of the brain. Such interconnections and interactions determine the information that brain regions have access to and the influence they exert.

In the current study we used diffusion-weighted MRI (DW-MRI) parcellation techniques to test the former hypothesis: the potential existence of new areas in humans. DW-MRI identifies areas corresponding in position and extent to those identified by histological examination (Mars et al., 2011). Another noninvasive MRI-based technique, resting-state fMRI, was used to explore the latter hypothesis—that there are interspecies differences in the functional networks vlFC participates in ("functional connectivity" [Bullmore and Sporns, 2009]). Functionally connected networks observed at rest often overlap with networks observed during performance of cognitive tasks (Power et al., 2011). Such interregional coupling patterns often partly reflect anatomical connectivity (O'Reilly et al., 2013). Previous studies have shown that dorsal prefrontal and parietal cortex participate in similar networks in macaques and humans (Margulies et al., 2009; Mars et al., 2011; Sallet et al., 2013; Vincent et al., 2007). Here we tested whether this is true in vlFC.

RESULTS

The first goal was to identify component parts of the entire human ventrolateral prefrontal cortex (Figure 1A). There has

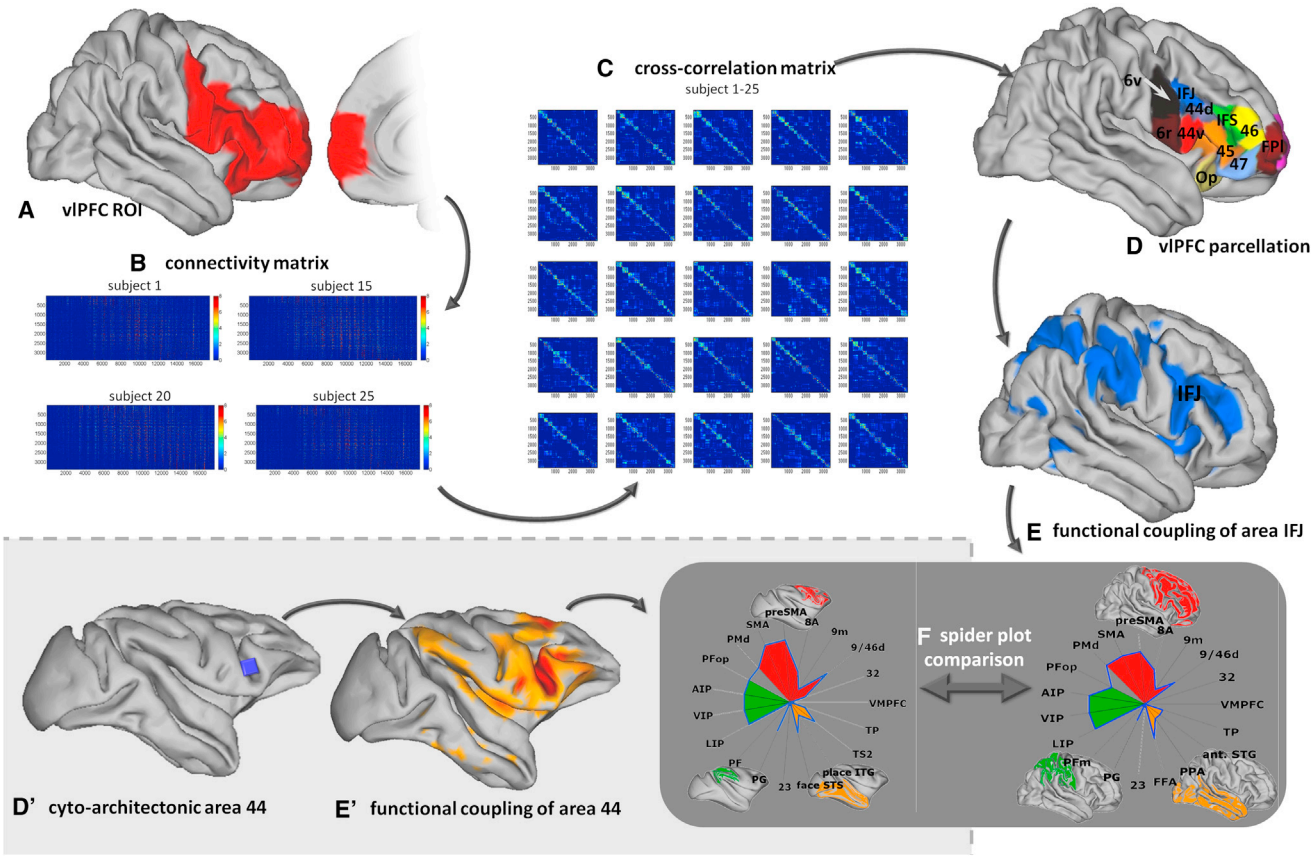

Figure 1. Overall Approach of the Study

We used DW-MRI-based tractography in 25 human participants to divide vlFC ROI (A) into regions with consistent connectivity profiles with the rest of the brain. Probabilistic tractography was performed from each voxel in the ROI and yielded a connectivity matrix between all VLFC voxels and each brain voxel for each participant (25 connectivity matrices, four example connectivity matrices in B). These matrices were then used to generate a symmetric cross-correlation matrix, which was then permuted using k-means segmentation for automated clustering to define different clusters (yielding 25 clustered cross-correlation matrices, C). These clusters were projected back onto the individual participant's brain and overlayed onto the MNI152 standard brain (D). fMRI analyses in the same 25 participants determined functional connectivity between these distinct vlFC regions and the rest of the brain (example functional connectivity pattern for IFJ in blue in E). We related the functional connectivity fingerprints (F) of the different vlFC regions to the resting-state fMRI-based connectivity profiles from different cytoarchitectonically defined areas in vlFC in 25 macaques (cytoarchitectonically defined macaque's area 44, D′, and respective functional connectivity pattern, E′).

recently been interest in the existence of specialized brain areas near the border between ventrolateral prefrontal and ventral premotor cortex (PMv). To ensure the possibility of investigating them in our study, we took care to include PMv as well as ventrolateral prefrontal cortex within the vlFC region of interest (ROI; see Figure 2A). Posteriorly, we delimited the ROI by the posterior end of the precentral gyrus to include the crown of the precentral gyrus but not the rostral bank of the central sulcus. Posterior to the posterior end of the inferior frontal sulcus, the ROI was dorsally delimited by what had previously been established to be the border between PMv and dorsal premotor cortex (PMd) (Tomassini et al., 2007). In addition to PMv, we also examined all areas in the pars opercularis, pars trianguris, and pars orbitalis of the inferior frontal gyrus, the whole of the inferior frontal sulcus, and the deep frontal operculum. Hence our ROI was delimited dorsally by the fusion of the middle frontal gyrus and the inferior frontal sulcus to include the whole inferior frontal sulcus. More anteriorly, we included all the tissue ventral to a line extending anteriorly from the anterior tip of the inferior frontal sulcus to the most anterior point in the brain. This line ran along the surface of the brain approximately in the axial plane in the standard Montreal Neurological Institute (MNI) coordinate system. Thereby, we probably included part of the frontal pole in this most anterior area, and for reasons of completeness we also included a more dorsal region into our ROI identified as frontal pole by Sallet et al. (2013). The ROI included both medial and lateral frontal pole and was medially delimited by the paracingulate sulcus. Ventromedially, the ROI was delimited by the lateral orbital sulcus and more posteriorly at the level of the deep frontal operculum by the circular sulcus. The ROI could be defined in an unbiased and easily reproducible way in all subjects by using the automated gray matter-white matter segmentation tool FAST v4.1 (FMRIB's Automated Segmentation Tool) (Zhang et al., 2001) on the MNI standard brain template (MNI_152 template) in combination with these gross anatomical

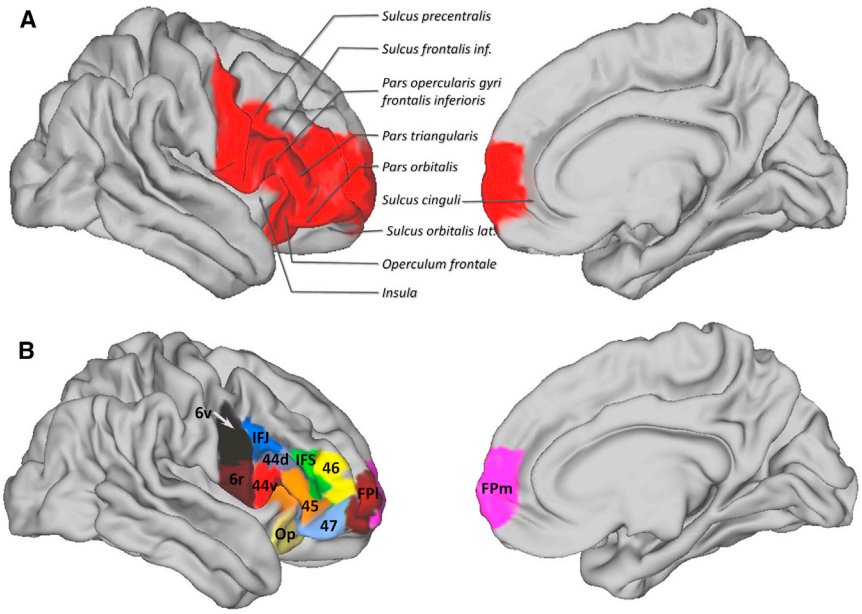

Figure 2. Human vlFC Region of Interest and Parcellation Solution

(A) The right vlFC ROI. Dorsally it included the inferior frontal sulcus and, more posteriorly, it included PMv; anteriorly it was bound by the paracingulate sulcus and ventrally by the lateral orbital sulcus and the border between the dorsal insula and the opercular cortex.

(B) A schematic depiction of the result of the 12 cluster parcellation solution using an iterative parcellation approach. We subdivided PMv into ventral and dorsal regions (6v and 6r, purple and black). We delineated the IFJ area (blue) and areas 44d (gray) and 44v (red) in lateral pars opercularis. More anteriorly, we delineated areas 45 (orange) in the pars triangularis and adjacent operculum and IFS (green) in the inferior frontal sulcus and dorsal pars triangularis. We found area 12/47 in the pars orbitalis (light blue) and area Op (yellow) in the deep frontal operculum. We also identified area 46 (bright yellow), and lateral and medial frontal pole regions (FPl and FPm, ruby colored and pink). See also Figures S1–S3 and S5.

landmarks. This standard-space ROI was then registered to each individual brain using nonlinear registration (FMRIB's Nonlinear Image Registration Tool [FNIRT]).

Because of potential differences between right and left vlFC, we carried out parallel investigations of both regions defined by the same anatomical criteria. However, we judged results to be similar enough to focus on right vlFC and to present left vlFC results only in the Supplemental Information.

To identify component vlFC regions, we used DW-MRI-based tractography in 25 healthy human participants. We estimated the connections of every vlFC voxel in each subject (Behrens et al., 2007) (Figure 1B). The parcellation approach identifies voxels within vlFC (Figure 1A) with similar estimated profiles of connectivity with the rest of the brain. The connectivity matrix (Figure 1B) is used to generate a symmetric cross-correlation matrix (Johansen-Berg et al., 2004) reflecting the correlation in connectivity pattern between all vlFC voxels. This cross-correlation matrix is then regrouped using K-means clustering (Figure 1C) to identify voxels sharing connectivity profiles (Beckmann et al., 2009; Mars et al., 2011). The spatial locations of the voxels in each parcel are then established; voxels cluster into anatomically coherent parcels (Figure 1D).

With the correct number of regions in human vlFC being unknown, we carried out a series of parcellations into two to 25 regions. The parcellation into ten distinct regions was particularly consistent across subjects and showed the smallest variance of the average cross-correlation, suggesting that it is the most coherent clustering into similarly correlated clusters (Supplemental Experimental Procedures 2 discusses determination of regions). Similar ten-cluster parcellations were obtained in both left and right hemispheres. This specific parcellation solution of ten different regions was further corroborated with a second series of parcellations using an iterative procedure (Supplemental Experimental Procedures 4) similar to the approach used by Beckmann et al. (2009). This iterative parcellation procedure yielded similar ten cluster results. Each of these ten regions was subsequently subjected to further subparcellation to test whether a more detailed parcellation of vlFC could be obtained. Two of the ten vlFC regions could reliably be parcellated further into two regions. Therefore, in summary, we identified 12 similar vlFC regions in all our human subjects.

The names given to each vlFC region need to be considered with caution. One strategy is to avoid naming areas, but we found this approach renders our findings difficult to communicate. Instead, we used names largely based on cross-species similarities in the areas' connectivity profiles. In several, but not all cases, they can be related to previous cytoarchitectonic and receptor-density-based parcellation schemes (Amunts et al., 2010).

After parcellation, we used fMRI from the same 25 humans to determine functional connectivity profiles for each vlFC region. We took the BOLD signal from each area and established which other voxels had correlated BOLD time courses (Figure 1E shows the example case of areas where the BOLD signal was correlated with the inferior frontal junction [IFJ] BOLD signal). We then summarized each vlFC area's pattern of coupling in a spider plot (Figure 1F). The spider plot shows the relative degree of coupling between each vlFC area and a set of target regions. These target regions were chosen because they are thought, on the basis of anatomical and functional evidence, to correspond between humans and macaques and because different vlFC areas were expected to have diagnostically different coupling patterns with different sets of these target regions. Similar spider plots were calculated for a set of macaque vlFC regions (Figure 1D′) and the corresponding target areas in other parts of the brain (Figure 1E′). Finally (Figure 1F), we compared the dissimilarity or "distance" between each human frontal area's coupling fingerprint and the coupling fingerprint associated with each frontal area of the macaque (Mars et al., 2013; Sallet et al., 2013).

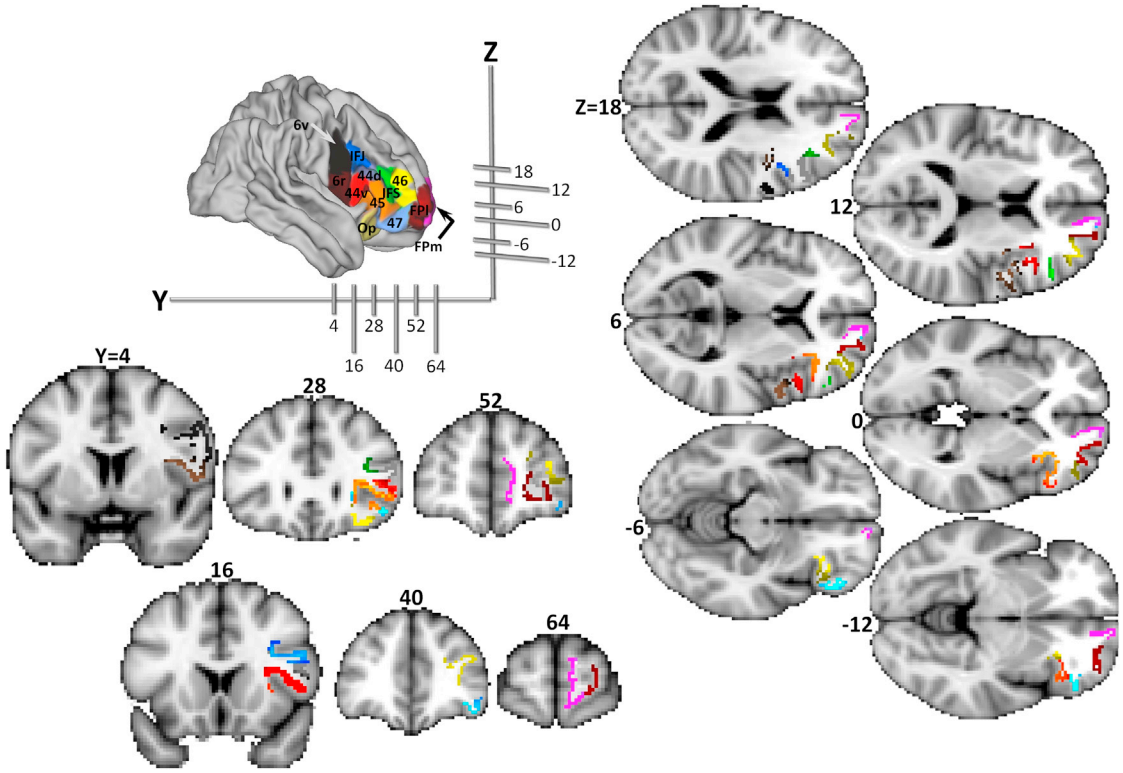

Figure 3. Human vlFC Parcellation Solution

Six coronal and six axial slices through the MNI152 standard brain as provided by FSL with the 12 vlFC subregions obtained by the tractography-based parcellation overlayed. The z and y coordinates for the respective slices are depicted next to the gray axes, which show the approximate location these slices were taken from.

Regions in Ventral Premotor Cortex

The human precentral gyrus territory overlapping with PMv (Tomassini et al., 2007) was subdivided into dorsal and ventral regions (brown and black, Figures 2B and 3; Supplemental Experimental Procedures 3) with centers of gravity at [x = 51, y = 1, z = 33] and [48, 5, 12] in MNI standard space, respectively. Given their topographical location, these areas probably correspond to the cytoarchitectonically defined agranular 6v and dysgranular 6r areas, although the ventral region extended into the operculum and therefore probably included parts of op6 (Amunts et al., 2010).

Human 6v and 6r (Figure 4) were similar in their functional connectivity. Both showed strong coupling to motor cortex, primary somatosensory cortex (S1), supplementary motor area (SMA), cingulate motor areas (CMAs), and PMd. Area 6r had stronger coupling with visuomotor areas including 7m, intraparietal sulcus (IPS), and anterior inferior parietal lobule (IPL), whereas 6v had stronger coupling with somatosensory regions, such as S1 and anterior parietal operculum, and with PMd. Neither coupled with inferior temporal lobe, suggesting that their visual information is mainly derived from parietal cortex.

There has been speculation about potential similarities of these regions in humans and macaques (Amunts et al., 2010; Belmalih et al., 2009; Rizzolatti and Sinigaglia, 2010). We found that functional connectivity patterns of macaque areas F5c and F5a resembled those of human areas 6v and 6r, respectively, and so below we refer to them collectively as 6v/F5c and 6r/F5a.

Pars Opercularis and Inferior Frontal Junction

We identified four subdivisions directly anterior to the precentral gyrus. The first occupied the posterior inferior frontal sulcus at its junction with the precentral sulcus (blue, Figure 2B) and had a center of gravity at [41, 12, 25]. This subdivision overlaps with the territory that has been called IFJ (Brass et al., 2005). Although our analyses demonstrated that IFJ can be reliably distinguished from adjacent vlFC areas, it remained a possibility that our IFJ region was not truly a separate region but just the most ventral extension of a more dorsal frontal area such as area 8A. To test this possibility, we created an ROI composed of IFJ and of area 8A (as defined by Sallet and colleagues, 2013) and subjected it to further parcellation attempts. In all subjects, we found that this larger ROI could be parcellated into two regions corresponding to IFJ and to area 8A, suggesting that the two areas are distinct (Figure S5).

Another more ventral region was located in lateral pars opercularis with a center of gravity at [41, 19, 10]. It posteriorly bordered F5a/6r. It therefore probably corresponds to area 44 (Amunts et al., 2010). Unlike almost all other areas that we investigated, we found that this area could be reliably subparcellated into dorsal and ventral subcomponents with centers of gravity at

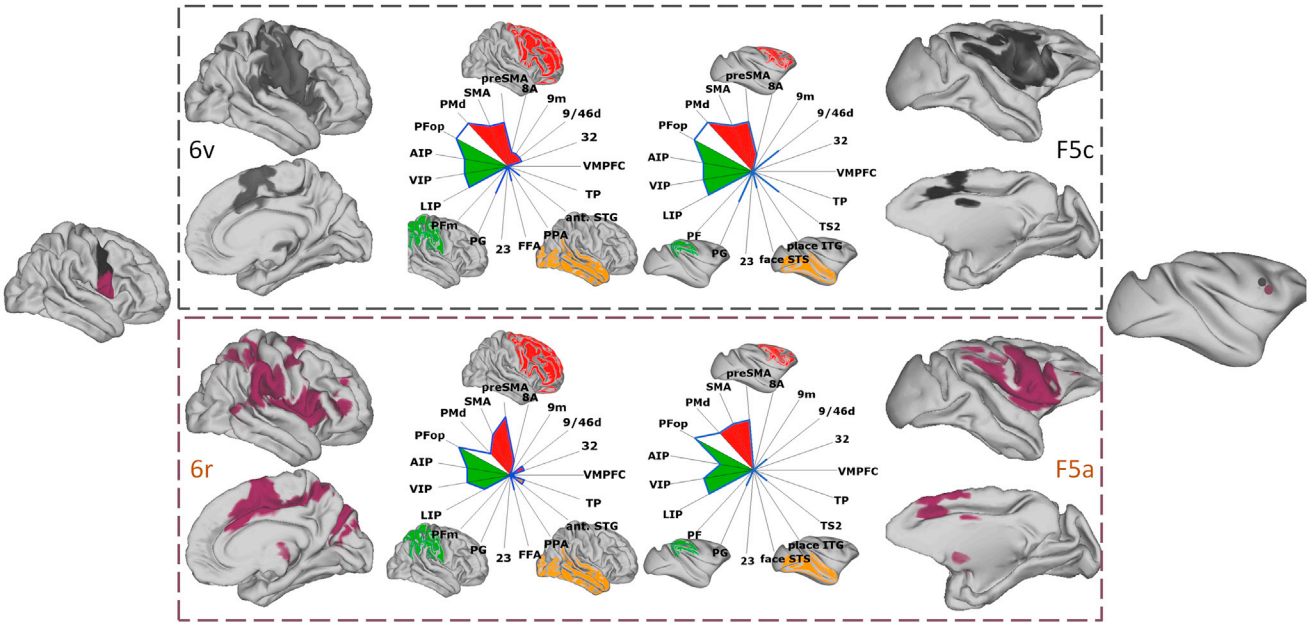

Figure 4. Regions in Ventral Premotor Cortex

Resting-state fMRI-derived functional connectivity patterns of human (left) areas 6v (black) and 6r (brown), which resemble those of macaque (right) areas F5c (black) and F5a (brown). In the middle, we show the intensities of these human and macaque resting-state fMRI-derived functional coupling patterns in a selected number of target ROIs that can be easily matched between the two species plotted on a spider plot. These spider plots were used to match human and monkey vlFC subregions. See also Figures S4 and S6.

[45, 23, 19] and [39, 20, 10] in all subjects. On the basis of their location, we suggest that they correspond to 44v and 44d (Amunts et al., 2010), although 44v extended into the operculum and therefore probably included parts of op8.

A fourth region was established in the middle section of the inferior frontal sulcus at [43, 32, 15] (green, Figure 2B). It bordered IFJ and 44d posteriorly, area 46 anteriorly, 44v inferiorly, and area 45 in the pars triangularis. This region is located in a similar region to the inferior frontal sulcus regions IFS1 and IFS2 (Amunts et al., 2010), and so we refer to it here as IFS.

Although our analyses demonstrated that IFS can be distinguished from other vlFC areas, it is still possible that IFS is not a truly separate region but just the most ventral part of a dorsal frontal cortical area such as area 9/46v. To test this possibility, we created an ROI composed of IFS and of area 9/46v (as defined by Sallet and colleagues, 2013) and subjected it to further parcellation attempts. In all subjects we found that this larger ROI could be parcellated into two regions corresponding to IFS and area 9/46v, suggesting that the two areas are distinct. We were not, however, able to reliably subdivide IFS into smaller component areas (Figure S4).

Examination of functional coupling suggested two important differences in the networks in which these four more anterior regions IFJ, 44d, 44v, and IFS participated, which contrasted with F5c/6v and F5a/6r network patterns. A related pattern of differences was found in macaque vlFC (Figure 5). Although all four regions remained coupled with F5c/6v and F5a/6r, they were also coupled with, first, a number of dorsolateral prefrontal areas and, second, visual association areas in occipitotemporal cortex.

Although the occipitotemporal areas do not appear in the spider plots in Figure 5, this coupling pattern is apparent in the rest of Figure 5. Occipitotemporal areas are absent from the spider plots because the spider plots focused on regions for which there is clear evidence of human-macaque correspondence (see Experimental Procedures and Table S3 for detailed account and references to cross-species homology of spider plot target areas); obviously, it is only the coupling with such areas that can be used to precisely decide how similar a vlFC area's functional network is in the two species, but such correspondences remain uncertain in occipitotemporal cortex. In macaque, these areas included V4, TEO, TE, and TPO.

The coupling of IFJ in humans suggests it occupies a transitional location between premotor and prefrontal cortex, distinguishing it from the more caudal premotor cortex that has little coupling with prefrontal cortex. To date, there has been no direct comparison of these human precentral subdivisions and areas in the macaque using the same technique. We found that a macaque vlFC region could be identified with a similar coupling profile—area 44 in the fundus of the inferior limb of arcuate sulcus. In contrast, the pattern of coupling of human 44v, with comparatively little interaction with parietal cortex, most closely resembled that of macaque area ProM. The coupling pattern of region 44d, which sits in between IFJ and 44v, bore broad similarities with the coupling pattern of IFJ. So we suggest that this region, like IFJ, may correspond to area 44 in the macaque. Nevertheless, it was notable that some aspects of 44d's coupling pattern were also reminiscent of 44v. Finally, the functional connectivity profile of human IFS resembled that of macaque area 45B.

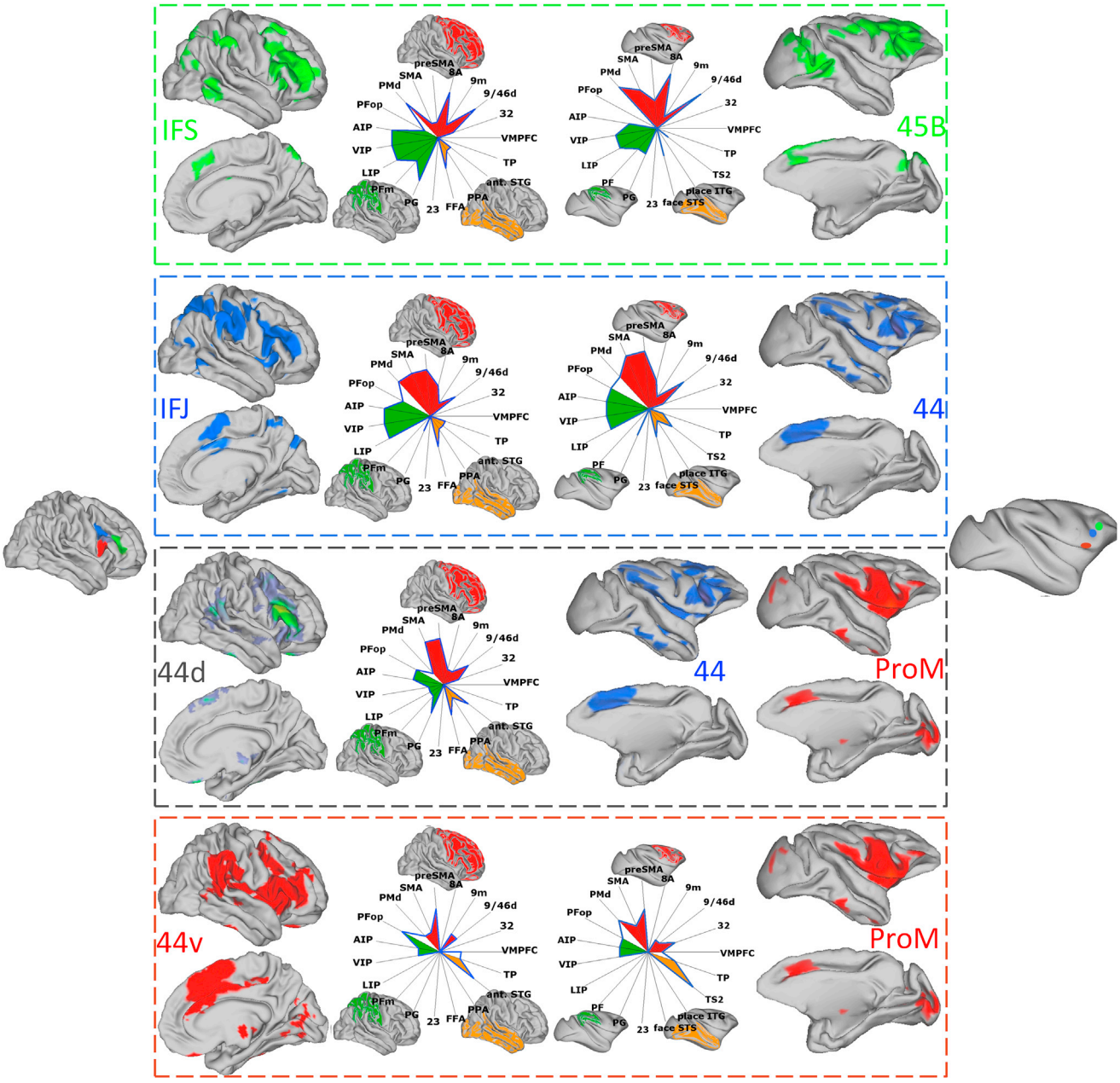

Figure 5. Pars Opercularis, Inferior Frontal Junction, and Inferior Frontal Sulcus

Resting-state fMRI-derived functional connectivity patterns of human areas IFS (green), IFJ (blue), 44d (green-gray), and 44v (red) and resting-state fMRI-derived functional coupling patterns of the proposed corresponding areas in macaque: areas 45B (green), 44 (blue), and ProM (red). Human area 44d resembled both macaque area 44 and ProM. In the middle, we show spider plots of these regions. Conventions are as in Figure 2. See also Figure S10.

The same cognitive control and language processes have been associated with both IFJ and 44v (Aron, 2007; Brass et al., 2005; Friederici and Gierhan, 2013), but our parcellation and functional connectivity results suggest that they have quite separate identities. To better understand the subdivisions we identified here, we related the functional coupling patterns of IFJ, 44v, and 45 (see below)—three regions that have particularly been implicated in language and cognitive control—to meta-analysis and derived coactivation patterns for several different cognitive tasks (Supplemental Experimental Procedures 6 and Figure S9a). Consistent with their different coupling profile, the meta-analysis suggested that these regions were associated with quite different functional roles, with area 44v involved in lower-level control processes seen in typical inhibition tasks such the go/no-go task and IFJ involved in higher-level processes such as task switching. Another region sometimes

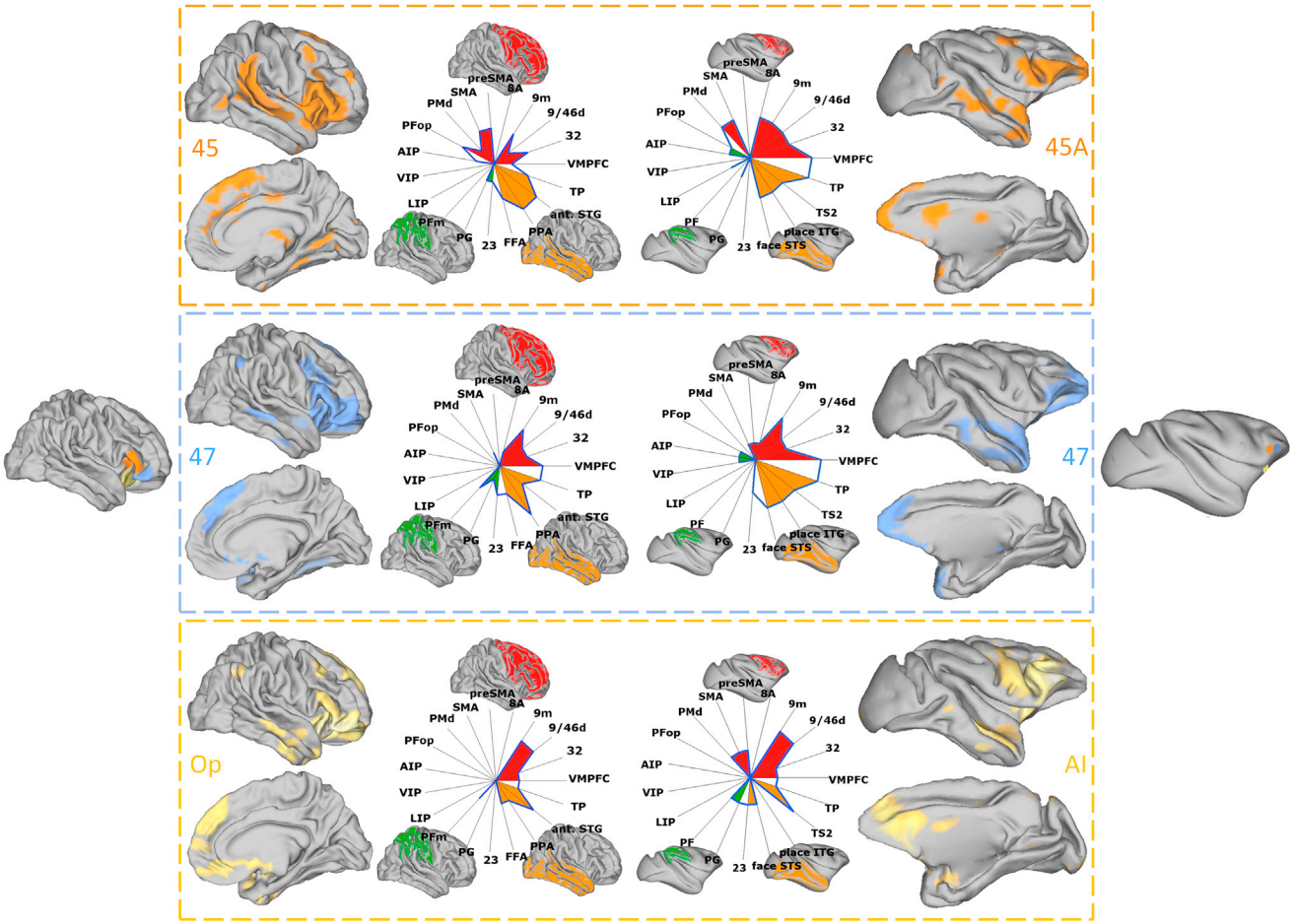

Figure 6. Pars Triangularis and Orbitalis

Resting-state fMRI-derived functional connectivity patterns of human areas 45 (orange), 12/47 (light blue), and Op (light yellow), and resting-state fMRI-derived functional connectivity patterns of the proposed corresponding areas in macaque (right): areas 45A (orange), 12/47 (light blue), and Op (light yellow). In the middle, we show spider plots of these regions. Conventions are as in Figure 2.

associated with inhibitory processes, area 45, was not associated with either of these functions but was rather implicated in social and language processes. Thus, the distinct coupling patterns of the human IFJ, 44v, and 45 accord with the distinct roles they play in language and cognitive control.

Pars Triangularis and Orbitalis

A more anterior vlFC region covered much of pars triangularis and the adjacent operculum with a center of gravity at [38, 29, −1] (orange, Figure 2). This subdivision seems to partly overlap with territory previously identified as 45 (Anwander et al., 2007) or, perhaps more precisely, 45A. We subsequently call this area 45 although it does not perfectly overlap with BA45 as defined by (Amunts et al., 1999). However, its location with respect to the other areas and its coupling pattern (see below) resemble area 45 (Petrides and Pandya, 2009). Another area was found in pars orbitalis and adjacent deep frontal operculum. This region is the second one in which it was possible to conduct further subparcellation into areas that had a consistent location in all subjects. One area was located on the gyrus of the pars orbitalis (cyan, Figure 2) with a center of gravity at [42, 34, −7] and therefore probably corresponds to area 47 or 47/12 (Petrides and Pandya, 2002), while the other area was in the deep frontal operculum with a center of gravity at [31, 26, −15] (bright yellow in Figure 2). This area is adjacent to areas that Amunts and colleagues (2010) refer to as Op9 and Op10 and partly overlaps with a region referred to as the frontal operculum by Higo et al. (2011). We use "Op" when referring to it in our human subjects.

In their functional coupling profiles, human area 45 and 47/12 most closely resembled macaque 45A and 47/12, respectively. Functional coupling patterns of human and macaque areas 45/45A and 47/12 shared common features such as coupling with other prefrontal areas and with temporal areas (Figure 6). In this they resembled the immediately posterior regions (IFJ/44d [human]/44 [macaque] and 44v/ProM). However, there was little evidence of coupling with action selection regions in parietal and premotor cortex. The main difference between 45 and 47/12 was that the latter was more closely linked to anterior parts of both temporal and prefrontal cortex in both species. The functional coupling profile of human Op most resembled the functional

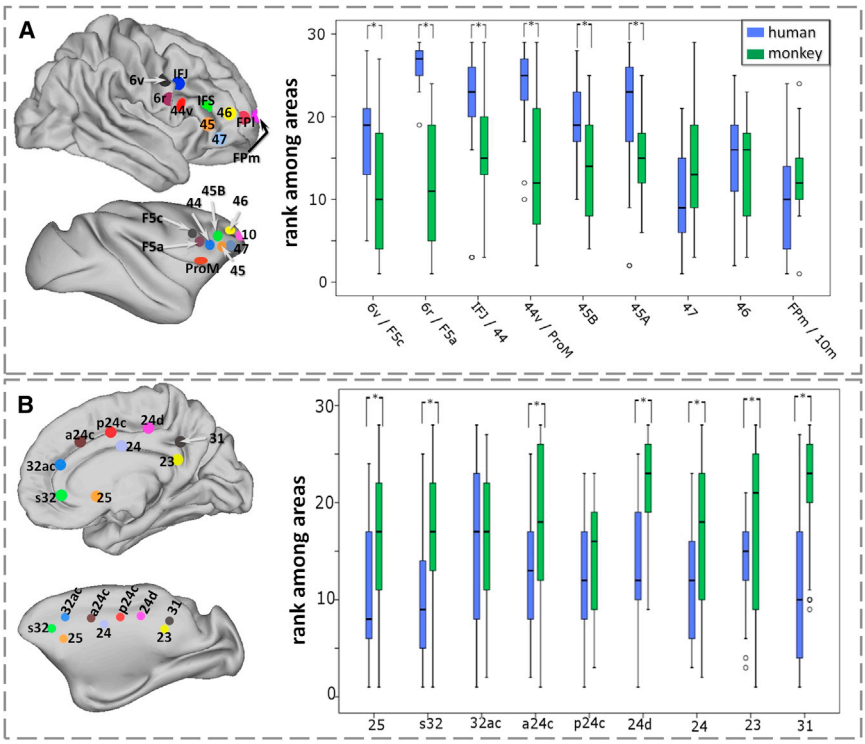

Figure 7. Human-Macaque Differences in Posterior Temporal Cortex Connectivity

fMRI-derived functional connectivity of a posterior auditory association area in the human and macaque (area Tpt) with region vlFC areas (A) and cingulate cortex (B). Graphs show the ranking of functional connectivity with the vlFC and cingulate areas in macaques and humans among all ROIs presented in spider plots in Figures 4, 5, and 6. The average intensity in the respective ROI from the seed-based correlation analysis z maps was rank ordered from lowest to highest values (i.e., high ranks reflect strong functional coupling) in two separate ranking analyses (one for auditory-vlFC coupling strength and a second for auditory-cingulate coupling strength). Asterisks mark significant between-species differences (Mann Whitney Wilcoxon rank-sum test; $p < 0.05$). See also Figures S7–S9.

coupling profile of the lateral agranular insula (Ial and Iapl in Carmichael and Price, 1994) in the macaque. Both human Op and macaque Ia were coupled with inferior and superior temporal cortex, perirhinal cortex and temporal pole, amygdala, and anterior dorsomedial frontal cortex.

Human-Macaque Differences in Posterior Temporal Cortex and Intrinsic vlFC Connectivity

Thus far, we have reported striking similarities between species. In both species, posterior ventral frontal cortex is coupled with sensorimotor regions important for action selection, while anterior vlFC is coupled with temporal visual association cortex. Such a combination suggests that, in both species, vlFC is well placed to categorize, select, and determine the flexible and often context-dependent influence visual representations have over decision making and action selection. Despite evidence for these similarities, we also observed major differences, most prominently in coupling with auditory areas. In humans, there was coupling between auditory association areas in posterior superior temporal cortex and many vlFC areas (Figure 7, Figures S6 and S7). This coupling was not limited to areas traditionally implicated in language but was apparent throughout 6v, 6r, 44v, IFJ, 44d, 45, and IFS. In macaques, this coupling was meager.

It might be argued that for some reason our scanning acquisition or analysis procedures were insensitive to long-range coupling between auditory association cortex and frontal lobes in macaques. This, however, cannot be the case, as we identified coupling of the same macaque posterior auditory association regions with medial prefrontal and anterior cingulate cortex (ACC) regions that are concerned with social interaction (Chang et al., 2013; Rudebeck et al., 2006) (Figure 7).

In fact, there is a "double dissociation" in posterior superior temporal-frontal lobe coupling in the two species; in macaques, posterior superior temporal coupling was strongest with medial frontal cortex, while in humans it was strongest with vlFC.

We also looked at vlFC intrinsic functional coupling to establish whether there was any between-species difference in the coupling of regions within vlFC (see Figure S8 and Supplemental Experimental Procedures 8). We noted less coupling between the two regions situated in PMv (6v/F5c–6r/F5a) for the human as compared to the macaque. We also found less coupling between 6r/F5a and 44v/ProM in human compared to macaques. However, we found stronger coupling between 44v and IFJ in the human compared to ProM and 44 in the macaque. We also found stronger coupling for 45B/IFS with 45, 45 with 47, and 44v/ProM with 46 in the human compared to the corresponding areas in the macaque (see Figure S8 with Figure S8A showing the functional coupling in human vlFC; white asterisks indicate significantly less and black asterisks significantly more functional coupling in human as compared to macaque). In summary, interregional coupling within prefrontal areas appeared stronger in humans than macaques, but the opposite was true for ventral premotor areas.

Areas in the Anterior Prefrontal Cortex

Three areas were identified in anterior human prefrontal cortex. One, on the edge of the investigated region, was actually in dorsolateral prefrontal cortex and corresponds to area 46 (yellow, Figure 2), with a center of gravity at [33, 47, 13], and has also been described elsewhere (Sallet et al., 2013). Two areas were delineated in the frontal pole (ruby and pink, Figure 2) with centers of gravity at [13, 59, 2] and [26, 54, 0]. We refer to them as medial and lateral frontal pole (FPm and FPl).

Human area 46 matched macaque area 46 in its functional connectivity. Like other vlFC areas, both were coupled with the frontal-parietal networks but the coupling was more limited in this

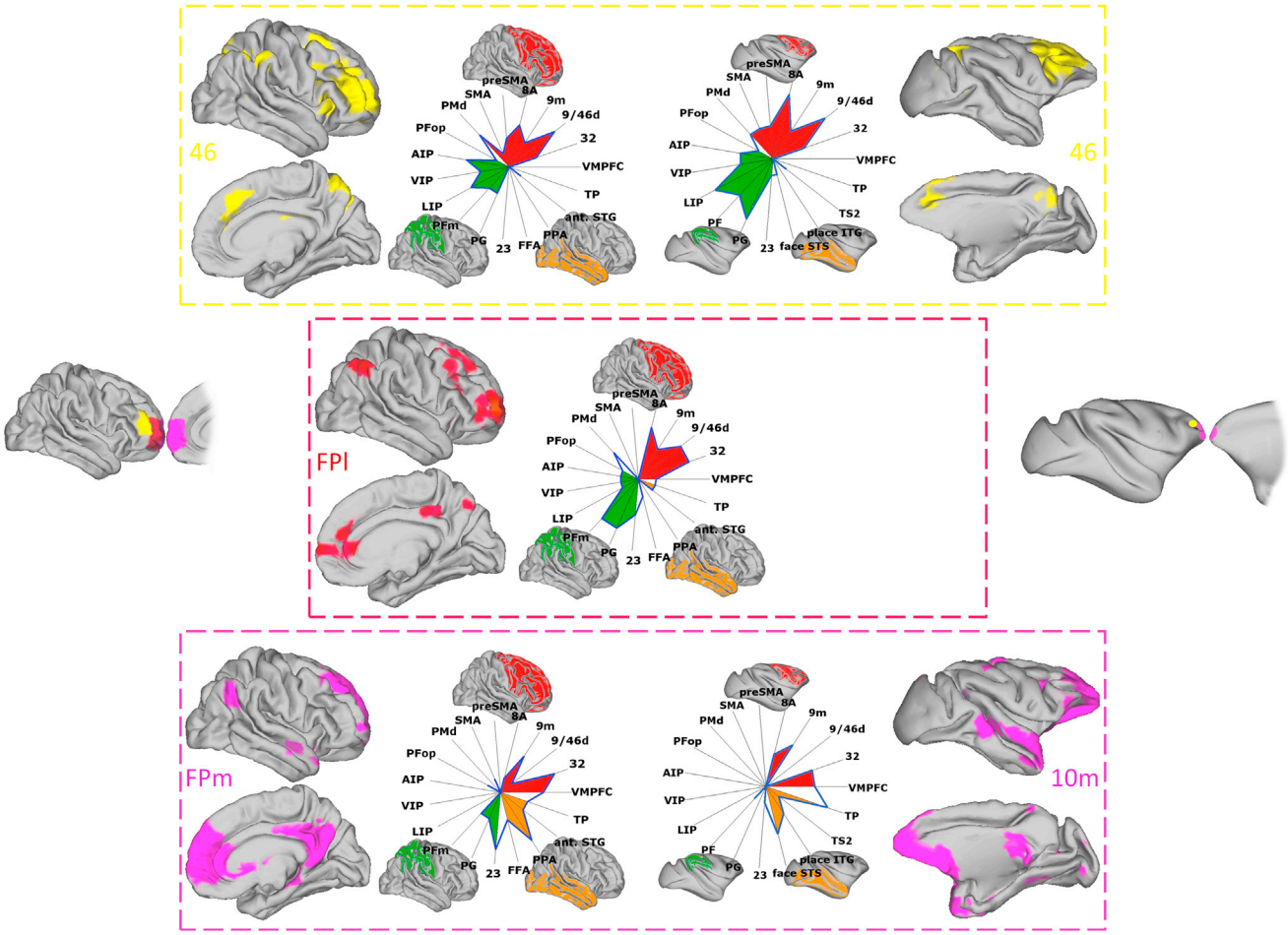

Figure 8. Areas in the Anterior Prefrontal Cortex

Resting-state fMRI-derived functional connectivity patterns of human (left) areas 46 (yellow), FPl (ruby), and FPm (pink), and resting-state fMRI-derived functional connectivity patterns of the proposed macaque correspondents (right): area 46 (yellow) and area 10 m (pink). Area FPl could not easily be matched to any macaque vlFC region but had some features of area 46. In the middle, we show spider plots of these regions. Conventions are as in Figure 2.

case. For example, in both humans and macaques, parietal coupling was strongest in IPL as opposed to IPS. The functional connectivity patterns of FPm and FPl (Figure 8) are distinct and only FPm corresponded in direct and simple ways to a macaque prefrontal brain region—the macaque's frontal pole region 10—while FPl did not. In both humans and macaques, FPm/10 were dramatically different to area 46 in that they showed little coupling with parietal cortex but instead, and unlike 46, they coupled with temporal pole, posterior cingulate cortex, and amygdala. These clear differences in coupling patterns of FPm/10 and 46 resemble differences in their connection patterns known from track-tracing experiments (Petrides and Pandya, 2007).

The coupling pattern of FPl bore little resemblance with that of FPm/10 but it rather partly resembled that of area 46; like area 46 it was coupled with IPL, and unlike FPm/10 it was not coupled with amygdala or temporal pole. However, FPl's coupling pattern was not identical to that of area 46; its IPL coupling was much more restricted than area 46's and indeed most of PFl's coupling was just with other prefrontal regions. In summary, human prefrontal cortex contains a region, FPl, that lacks simple correspondence with any in macaque prefrontal cortex. FPl does not show those coupling patterns that are usually distinctive features of FP cortex, but it instead exhibits coupling patterns reminiscent of dorsolateral prefrontal cortex.

DISCUSSION

We identified fundamental similarities but also striking differences between monkeys and humans in the way vlFC regions link with the rest of the brain. We discuss these results in four parts, focusing briefly on (1) PMv, then (2) posterior vlFC areas associated with cognitive control, (3) vlFC areas and their hypothesized role in language processing in humans, and (4) areas in the most anterior part of the prefrontal cortex.

Ventral Premotor Cortex

Previous studies have dissociated PMd from PMv using DWI-tractography-based estimates of connectivity (Tomassini et al.,

2007). Here we show further dissociation between superior and inferior regions within human PMv that we refer to as 6v and 6r. A related distinction has also been proposed by Schubotz et al. (2010). These areas' functional connectivity patterns resemble those of macaque areas F5c and F5a, respectively. There was functional coupling between both areas in both species and coupling with anterior intraparietal area (AIP), pre-SMA, and parts of ventral prefrontal cortex. Connections between these areas have previously been reported in tracer injection studies (Borra et al., 2011; Luppino et al., 1999). Further subdivision of area 6v, which lies on the edge of the ROI we investigated, may be possible; the existence of coupling between 6v and ventral intraparietal area (VIP) and SMA resembled the anatomical connections of macaque area F4 that are known to exist (Luppino et al., 1999).

Macaque F5 hosts "canonical neurons" encoding specific object-oriented action plans and affordances as well as "mirror neurons" that are active both when monkeys perform object-oriented actions and when they observe the same actions (Belmalih et al., 2009). More posterior F5c may represent actions performed in a context-dependent way, while F5a may code actions at a more abstract level (Nelissen et al., 2005). Such differences may be a consequence of differences in connectivity with parietal and other sensorimotor areas (Nelissen et al., 2011), which were also apparent in our study.

Posterior vlFC and Cognitive Control

Parts of posterior vlFC have been associated with cognitive control processes, including inhibitory motor control (Aron, 2007), cognitive task control (Dosenbach et al., 2006), cognitive flexibility (Brass et al., 2005), and information updating (Duncan and Owen, 2000). One of the first important results was that DWI-tractography parcellation reliably distinguished five areas—IFJ, 44d, 44v, Op, and IFS—from the surrounding cortex; this is from both the more posterior PMv and the more anterior and dorsal parts of prefrontal cortex. There has been interest in the possibility that regions of vlFC differ in terms of their involvement in various tasks of cognitive flexibility (Chikazoe et al., 2009; Verbruggen et al., 2010). The parcellation, functional coupling, and meta-analyses that we report here all suggest that the regions participate in different cognitive processes.

For all five areas, we identified areas in macaque vlFC that they resembled (Figures 5 and 6). Neurophysiological studies of cognitive control in macaques have focused on the principal sulcus region, but our results suggest that investigation of areas 44, Ia, and ProM might also shed light on the mechanisms of cognitive control.

For both species, the functional coupling patterns of these five regions participated in partly similar networks as premotor areas 6v/F5c and 6r/F5a, and indeed most were also coupled with 6v/F5c and 6r/F5a. From the similarity between the coupling patterns of these five areas and areas 6v/F5c and 6r/F5a, their involvement in action selection may be inferred. However, the additional and distinct coupling of IFJ, 44d, 44v, Op, and IFS with visual association areas in occipitotemporal cortex and dorsolateral prefrontal cortex suggested important differences in function. We propose that these five areas have more flexible control over action selection—by reference to information from dorsolateral prefrontal cortex about higher order goals and sequential information (Genovesio et al., 2012) and with access to richer descriptions of visual features from the temporal lobe that go beyond the action affordances encoded in parietal visuomotor neurons.

vlFC Areas Associated with Language

Although macaques lack language, we found regions in macaque vlFC that showed a pattern of functional coupling similar to human vlFC regions implicated in language. Human areas 45 and 47/12, which play roles in semantic processing, resemble macaque areas 45A and 47/12. We also found similar subdivisions in the human left and right hemispheres. Although Broca's area is only present in the left hemisphere, similarities in cytoarchitecture and receptor densities in the two hemispheres have been reported before (Amunts et al., 2010).

The development of abilities such as language may, therefore, have exploited pre-existing mechanisms for sensory-motor mapping (Rizzolatti and Sinigaglia, 2010), sequential motor learning (Koechlin and Jubault, 2006), or multimodal sensory integration (Passingham and Wise, 2012; Romanski, 2012).

Although we found similar coupling patterns with premotor and parietal cortex, we also noted pronounced species differences in how most vlFC regions coupled with posterior auditory association areas. Whereas macaque auditory association areas in the posterior temporal cortex coupled strongly with ACC areas known to play a role in social cognition (Rudebeck et al., 2006), human posterior auditory association areas coupled more strongly with almost all vlFC regions.

These striking discrepancies might relate not just to the prominence of auditory information in human language but even more generally to the poor ability of macaques to use auditory information for a range of purposes. For example, macaques perform poorly in auditory working memory tasks (Scott et al., 2012), and while they are readily able to learn to use visual information to guide arbitrary and flexible patterns of decision making, they find it difficult to use auditory information in the same way (Gaffan and Harrison, 1991). The ability that humans possess in using auditory and verbal codes to guide decision making and in short-term memory may depend on the coupling between posterior auditory association cortex and ventrolateral prefrontal cortex that only they, and not macaques, possess.

Anterior vlFC

Frontopolar cortex has been associated with representing future and alternative courses of action (Boorman et al., 2011; Koechlin, 2011). Its more medial part has been implicated in social cognition (Frith and Frith, 2007). In the present study, we subdivided it into lateral, FPl, and medial, FPm, subdivisions. Both were distinct from dorsolateral prefrontal area 46. Whereas human area 46 and FPm could be matched to macaque areas 46 and 10 on the basis of their functional connectivity, human area FPl could not easily be matched to any of the macaque prefrontal cortex (PFC) regions. This supports the notion that human anterior PFC contains a region not found in the macaque and suggests it may support distinctive cognitive abilities. One way in which new regions arise during speciation is as a consequence of connections normally associated with one area invading an adjacent area (Krubitzer, 2007). Human FPl's coupling pattern may reflect

such a process. The existence of a distinctive human FPl region may explain Mantini and colleagues (2013) recent finding of distinctive components in human fMRI activity patterns.

Comparison with Previous Studies

The ROI we investigated was defined on the basis of sulcal landmarks, but it corresponds approximately to the frontal and opercular component of the frontoparietal task control and the cingulo-opercular networks or the frontoparietal and ventral attentional networks that have been described previously (Power et al., 2011; Yeo et al., 2011).

Parcellation studies have previously identified areas 44 and 45 within human vlFC (Anwander et al., 2007; Klein et al., 2007). In this study, we were also able to identify ten other regions beyond areas 44 and 45 including a frontopolar region FPl unique to humans. With the exception of FPl, we were able to relate them to areas in the monkey brain.

Previous studies of human areas 44 and 45 have focused on estimating the probability that the areas are connected with a limited number of major white matter fascicles. By using similar resting-state BOLD coupling measures in both species, we estimated interaction strengths between each of our 12 vlFC regions and 19 other brain areas in specific regions of temporal, parietal, premotor, and cingulate cortex. This made it possible to show that human and macaque vlFC regions are fundamentally similar in their interactions with specific parietal, premotor, and cingulate regions and with visual association regions in temporal cortex but not with superior temporal auditory association cortex. VlFC circuits in humans and macaques differ in the manner in which they interact with an important part of auditory association cortex, but they greatly resemble each other in the manner in which they interact with visual, action-selection, and decision-making areas, thereby emphasizing the role of human vlFC, even human vlFC areas such as 44 and 45, in functions other than language.

Limitations

The DWI-tractography parcellation technique identifies reproducible distinctions between brain areas (Mars et al., 2011; Wang et al., 2012; Zhang et al., 2012) and areas that correspond with histologically defined brain areas, both in terms of their positions in standard MNI space and with respect to sulcal landmarks (Caspers et al., 2008; Mars et al., 2011; Scheperjans et al., 2008). This suggests that areas we identify here correspond to separable anatomical entities within vlFC that have a reliable location in standard MNI space. However, it is important to note that probabilistic DWI-tractography only estimates the strength of evidence for a connection and that there are both false positives and negatives in the connections it estimates (Dyrby et al., 2007; Johansen-Berg and Rushworth, 2009). However, the correspondence between DWI-tractography parcellation and histologically defined brain areas reflects the fact that the parcellation approach draws on estimates of connectivity between the ROI and every other voxel in the brain rather than just on estimates of connectivity with a single region or pathway that might be inaccurately characterized.

Other laboratories have attempted to parcellate human cortex on the basis of differences in functional connectivity measured with fMRI and there are similarities, albeit not complete ones, in the schemes that have been proposed using this approach (Margulies et al., 2009; Power et al., 2011; Yeo et al., 2011) and between such approaches and schemes employing DWI-tractography-based parcellation approaches (Mars et al., 2011; Nelson et al., 2010). This probably reflects the fact that functional coupling between any two brain areas is a function of the anatomical interconnections between the areas; functional coupling is reduced when direct anatomical connections between the areas are removed but only abolished when indirect anatomical connections are also removed (O'Reilly et al., 2013). Functional connectivity measurements have the advantage that they are less sensitive to interareal distance than are DWI measurements. By drawing on both DWI-tractography and fMRI connectivity, we have attempted to combine the strengths of each method but note that it cannot replace detailed anatomical investigation both in animal models and human tissue acquired postmortem (e.g., Amunts et al., 2010; Petrides and Pandya, 2007). Nevertheless, we hope that our results contribute to an understanding of how data derived from animal models can be used to aid understanding of human brain function.

EXPERIMENTAL PROCEDURES

Diffusion-Weighted Tractography-Based Parcellation

Diffusion-weighted images were acquired in 25 healthy right-handed participants on a 3 T Siemens Magnetom Verio MR scanner using standard DW-MRI protocols (Supplemental Experimental Procedures 1). Analyses were performed using tools from FSL (Functional MRI of the Brain Software Library), the Human Connectome Project Workbench, and custom-made software written in MATLAB (MathWorks). DW-MRI data were preprocessed in a standard way as previously described (Mars et al., 2011; Supplemental Experimental Procedures 2).

For each participant, probabilistic tractography was run from each voxel in the right vlFC ROI (the same steps were also performed for the left vlFC; Figure S3) to assess connectivity with every brain voxel (whole-brain "target" was down sampled after tractography to 5 mm isotropic voxels for the connectivity matrix to be manageable; however, the whole vlFC ROI was tracked in original FA space, see Figure 1), using a model accounting for multiple fiber orientations in each voxel (Behrens et al., 2007). A connectivity matrix between all right vlFC voxels and each brain voxel was derived and used to generate a symmetric cross-correlation matrix of dimensions (number of seeds × number of seeds) in which the (i,j) element value is the correlation between the connectivity profile of seed i and the connectivity profile of seed j. The rows of this cross-correlation matrix were then permuted using k-means segmentation for automated clustering to define different clusters (Figure 1C and Figure S1). The goal of clustering the cross-correlation matrix is to group together seed voxels that share the same connectivity with the rest of the brain. The parcellation into ten distinct regions was particularly consistent across subjects and showed the smallest variance of the average cross-correlation, suggesting the most coherent clustering into similarly correlated clusters (Supplemental Experimental Procedures 3 discusses determination of regions and concept of "brain region"). We carried out an additional analysis in which we iteratively parcellated vlFC into smaller and smaller regions and identified the same ten regions (Supplemental Experimental Procedures 4 and Figure S2). Using this approach, however, we showed that two of the areas could be subdivided, bringing the total areas identified to 12.

Human Resting-State fMRI Data Acquisition, Preprocessing, and Analysis

Human resting-state fMRI data were collected for the same group of 25 healthy volunteers in the same session using the same scanner. Participants were

instructed to lie still and keep their eyes open and fixated at a cross. Resting-state fMRI data acquisition and preprocessing were carried out in a standard way as previously described (Mars et al., 2011; Supplemental Experimental Procedures 5).

To establish the functional connectivity of each vlFC region, we created ROIs from every parcel in each individual subject's parcellation. As representation of each parcel, we took the 5% most likely voxels from each parcel's whole vlFC certainty maps (which in MNI space are always 170 voxels for a 3,400 voxel vlFC ROI) from the fuzzy-clustering-derived parcel-specific maps. The fuzzy-clustering algorithm gives a certainty of each voxel belonging to each of the clusters and hence provides a "certainty map" of the whole vlFC ROI for each cluster. Note however that we also tried extracting the time courses from each parcel as a whole from the "normal" k-means clustering and obtained largely similar resting-state functional connectivity patterns. Moreover, we drew cubic regions of interest (3 × 3 × 3 voxels, i.e., 6 mm isotropic) at the center of gravity of each individual subject's parcel and also at the center of gravity of each parcel in the group maps and obtained qualitatively similar results. Individual ROIs were registered from each subject's DW-MRI space into fMRI space using FLIRT. Then the major Eigen time series representing activity in each of the vlFC clusters was calculated.

Individual statistical maps were then calculated using a seed-based correlation analysis, which is part of FSL (fsl_sbca) as previously described (Mars et al., 2011; O'Reilly et al., 2010), in order to infer the functional connectivity of these ROIs with the rest of the brain. For each vlFC subdivision, we created a model consisting of the first Eigen time series of that region and the confounding time series representing head movement (six regressors resulting from motion correction using MCFLIRT) and the Eigen time series of white matter and corticospinal fluid (CSF). The results of each individual subject's ROI-specific seed-based-correlation analysis were then entered into a general linear model (GLM) analysis. The resulting z statistical images were thresholded using clusters determined by $z > 4.0$ and a (corrected) cluster significance threshold of $p < 0.05$. These thresholded group z maps were projected onto the CaretBrain as provided by the Human Connectome Project Workbench using the "surf_proj" algorithm as implemented in FSL and then visualized using the Human Connectome Project Workbench. Unthresholded z maps were quantified by extracting the average intensity of each cluster's functional connectivity z map in a number of cortical regions of interest (Tables S1, S2, and S3). We drew 3 × 3 × 3 voxels, i.e., 6 mm isotropic, ROIs centered on the coordinates mentioned in Table S1 and then averaged the z value from the unthresholded seed-based correlation analysis-derived z maps within these ROIs. These values for all ROIs and all vlFC areas were then binned into four equally sized bins. These were then displayed on a spider plot (Figures 4, 5, 6, and 8).

Macaque Resting-State fMRI Data Acquisition, Preprocessing, and Analysis

Resting-state fMRI and anatomical scans were collected for 25 healthy macaques (*Macaca mulatta*) (four females, age: 3.9 years, weight: 5.08 kg) under light inhalational anesthesia with isoflurane (for detailed information on anesthesia protocol, monitoring of vital signs, data acquisition, and preprocessing, see Supplemental Experimental Procedures 7). Protocols for animal care, MRI, and anesthesia were performed under authority of personal and project licenses in accordance with the United Kingdom Animals (Scientific Procedures) Act (1986).

The goal of this part of the study was to test for similarities between the functional networks previously established for human vlFC and vlFC regions in the macaque. We therefore aimed to map the resting-state functional connectivity networks of all cytoarchitectonically described areas in macaque vlFC and adjacent ventral premotor and insular areas. Functional connectivity networks of several regions (the lateral area 10, medial area 10, ventral area 10, area 46, area 9/46v, area 47/12, area 45A, area 45B, area 44, area 8A [Petrides and Pandya, 1999, 2002]; motor proisocortex [ProM], the anterior insula [Ai], and the gustatory area [Carmichael and Price, 1994]; areas F5a, F5c, and F5p [Belmalih et al., 2009]) were identified using a seed-based-correlation analysis, which is part of FSL (fsl_sbca), as in the human subjects, to infer the functional connectivity of these ROIs with the rest of the brain. The seed regions were specified in stereotactic atlases of the macaque monkey brain (Paxinos et al., 2000; Saleem and Logothetis, 2007) and then drawn on the standard brains of the respective atlas. They could then be registered between atlases using FLIRT.

Comparison of Resting-State Functional Connectivity of Macaque and Human vlFC

We identified the macaque regions most comparable to human vlFC regions in terms of functional connectivity. The functional connectivity between each vlFC area and 19 areas in the rest of the brain (each of which corresponded in both humans and macaques; Table S2) was plotted on spider plots for both species. The ROIs were 6 mm isotropic (coordinates in Table S1) for humans and 3 mm isotropic for macaques identified using stereotactic atlases of the macaque monkey brain and then drawn on the standard brains of the respective atlas. We then determined which macaque vlFC region corresponded most closely to each human vlFC. A formal comparison between human and macaque vlFC coupling patterns was performed by calculating the summed absolute difference (the "Manhattan" or "city-block" distance [Mars et al., 2013; Sallet et al., 2013]) of the normalized coupling scores after binning into four equally sized bins. This yielded a summary measure (Figure S6) of the difference in coupling patterns for each pair of areas in the two species. The summary measure can then be used to compare the functional coupling pattern of each human vlFC region with those of all vlFC regions in the macaque.

Functional Coupling of Visual and Auditory Association Regions with Regions in vlFC and Medial Frontal Cortex

To compare functional coupling between vlFC and auditory association cortex in posterior superior temporal cortex in humans and macaques, we rank ordered the strength of functional coupling (from lowest to highest) between area Tpt and ten vlFC areas that corresponded in both humans and macaques (average z value in cubic ROI 6 × 6 × 6 mm in human and 3 × 3 × 3 mm in macaque) among the 19 previously described target regions (same regions as in the spider plots). In other words, we assessed how strong the coupling between area and Tpt and each vlFC subregion ranked in comparison to coupling between Tpt and each of the other 19 areas (VMPFC, area 32, 9/46d, etc.). We then performed a Mann-Whitney-Wilcoxon rank-sum test (significance level $p < 0.05$), comparing the rank areas assigned to the coupling strength between each vlFC region and Tpt in the two species (Figure 7, Figure S8 presents the same analysis not only for area Tpt [left] but also for anterior auditory association area TS2, Figure S9 presents the same analysis for the left hemisphere).

Another analysis compared the functional coupling of area Tpt (Figure 7; for area TS2 see Figures S8 and S9) and nine cingulate cortex areas (Beckmann et al., 2009). This means that there were always 29 (vlFC) or 28 (cingulate) ROIs in each of the two separate analyses. The average z values in the target ROIs representing coupling of area Tpt with vlFC or cingulate areas were ranked for each individual and compared between species with a Mann-Whitney-Wilcoxon rank-sum test ($p < 0.05$ significance level). A rank of 29 (vlFC analysis) or 28 (cingulate analysis) was the highest possible rank (strongest coupling of an ROI among all 29/28 ROIs).

SUPPLEMENTAL INFORMATION

Supplemental Information includes Supplemental Experimental Procedures, ten figures, four tables, and neuroimaging files and can be found with this article online at http://dx.doi.org/10.1016/j.neuron.2013.11.012.

ACKNOWLEDGMENTS

This research was supported by Medical Research Council (United Kingdom) G0802146 (to M.F.S.R. and R.B.M.), a Gustav Born Scholarship (to F.-X.N.), and a Christopher Welch Scholarship (to F.-X.N.). We thank Vanessa M. Johnen for helpful comments on an earlier version of the manuscript.

Accepted: November 4, 2013
Published: January 28, 2014

REFERENCES

Amunts, K., Schleicher, A., Bürgel, U., Mohlberg, H., Uylings, H.B., and Zilles, K. (1999). Broca's region revisited: cytoarchitecture and intersubject variability. J. Comp. Neurol. *412*, 319–341.

Amunts, K., Lenzen, M., Friederici, A.D., Schleicher, A., Morosan, P., Palomero-Gallagher, N., and Zilles, K. (2010). Broca's region: novel organizational principles and multiple receptor mapping. PLoS Biol. *8*, 8.

Anwander, A., Tittgemeyer, M., von Cramon, D.Y., Friederici, A.D., and Knösche, T.R. (2007). Connectivity-Based Parcellation of Broca's Area. Cereb. Cortex *17*, 816–825.

Aron, A.R. (2007). The neural basis of inhibition in cognitive control. Neuroscientist *13*, 214–228.

Beckmann, M., Johansen-Berg, H., and Rushworth, M.F. (2009). Connectivity-based parcellation of human cingulate cortex and its relation to functional specialization. J. Neurosci. *29*, 1175–1190.

Behrens, T.E., Berg, H.J., Jbabdi, S., Rushworth, M.F., and Woolrich, M.W. (2007). Probabilistic diffusion tractography with multiple fibre orientations: What can we gain? Neuroimage *34*, 144–155.

Belmalih, A., Borra, E., Contini, M., Gerbella, M., Rozzi, S., and Luppino, G. (2009). Multimodal architectonic subdivision of the rostral part (area F5) of the macaque ventral premotor cortex. J. Comp. Neurol. *512*, 183–217.

Boorman, E.D., Behrens, T.E., and Rushworth, M.F. (2011). Counterfactual choice and learning in a neural network centered on human lateral frontopolar cortex. PLoS Biol. *9*, e1001093.

Borra, E., Gerbella, M., Rozzi, S., and Luppino, G. (2011). Anatomical evidence for the involvement of the macaque ventrolateral prefrontal area 12r in controlling goal-directed actions. J. Neurosci. *31*, 12351–12363.

Brass, M., Derrfuss, J., Forstmann, B., and von Cramon, D.Y. (2005). The role of the inferior frontal junction area in cognitive control. Trends Cogn. Sci. *9*, 314–316.

Bullmore, E., and Sporns, O. (2009). Complex brain networks: graph theoretical analysis of structural and functional systems. Nat. Rev. Neurosci. *10*, 186–198.

Carmichael, S.T., and Price, J.L. (1994). Architectonic subdivision of the orbital and medial prefrontal cortex in the macaque monkey. J. Comp. Neurol. *346*, 366–402.

Caspers, S., Eickhoff, S.B., Geyer, S., Scheperjans, F., Mohlberg, H., Zilles, K., and Amunts, K. (2008). The human inferior parietal lobule in stereotaxic space. Brain Struct. Funct. *212*, 481–495.

Chang, S.W., Gariepy, J.F., and Platt, M.L. (2013). Neuronal reference frames for social decisions in primate frontal cortex. Nat. Neurosci. *16*, 243–250.

Chikazoe, J., Jimura, K., Hirose, S., Yamashita, K., Miyashita, Y., and Konishi, S. (2009). Preparation to inhibit a response complements response inhibition during performance of a stop-signal task. J. Neurosci. *29*, 15870–15877.

Dosenbach, N.U., Visscher, K.M., Palmer, E.D., Miezin, F.M., Wenger, K.K., Kang, H.C., Burgund, E.D., Grimes, A.L., Schlaggar, B.L., and Petersen, S.E. (2006). A core system for the implementation of task sets. Neuron *50*, 799–812.

Duncan, J., and Owen, A.M. (2000). Common regions of the human frontal lobe recruited by diverse cognitive demands. Trends Neurosci. *23*, 475–483.

Dyrby, T.B., Søgaard, L.V., Parker, G.J., Alexander, D.C., Lind, N.M., Baaré, W.F., Hay-Schmidt, A., Eriksen, N., Pakkenberg, B., Paulson, O.B., and Jelsing, J. (2007). Validation of in vitro probabilistic tractography. Neuroimage *37*, 1267–1277.

Friederici, A.D., and Gierhan, S.M. (2013). The language network. Curr. Opin. Neurobiol. *23*, 250–254.

Frith, C.D., and Frith, U. (2007). Social cognition in humans. Curr. Biol. *17*, R724–R732.

Gaffan, D., and Harrison, S. (1991). Auditory-visual associations, hemispheric specialization and temporal-frontal interaction in the rhesus monkey. Brain *114*, 2133–2144.

Genovesio, A., Tsujimoto, S., and Wise, S.P. (2012). Encoding goals but not abstract magnitude in the primate prefrontal cortex. Neuron *74*, 656–662.

Higo, T., Mars, R.B., Boorman, E.D., Buch, E.R., and Rushworth, M.F. (2011). Distributed and causal influence of frontal operculum in task control. Proc. Natl. Acad. Sci. USA *108*, 4230–4235.

Johansen-Berg, H., and Rushworth, M.F. (2009). Using diffusion imaging to study human connectional anatomy. Annu. Rev. Neurosci. *32*, 75–94.

Johansen-Berg, H., Behrens, T.E., Robson, M.D., Drobnjak, I., Rushworth, M.F., Brady, J.M., Smith, S.M., Higham, D.J., and Matthews, P.M. (2004). Changes in connectivity profiles define functionally distinct regions in human medial frontal cortex. Proc. Natl. Acad. Sci. USA *101*, 13335–13340.

Klein, J.C., Behrens, T.E., Robson, M.D., Mackay, C.E., Higham, D.J., and Johansen-Berg, H. (2007). Connectivity-based parcellation of human cortex using diffusion MRI: Establishing reproducibility, validity and observer independence in BA 44/45 and SMA/pre-SMA. Neuroimage *34*, 204–211.

Koechlin, E. (2011). Frontal pole function: what is specifically human? Trends Cogn. Sci. *15*, 241, author reply 243.

Koechlin, E., and Jubault, T. (2006). Broca's area and the hierarchical organization of human behavior. Neuron *50*, 963–974.

Krubitzer, L. (2007). The magnificent compromise: cortical field evolution in mammals. Neuron *56*, 201–208.

Luppino, G., Murata, A., Govoni, P., and Matelli, M. (1999). Largely segregated parietofrontal connections linking rostral intraparietal cortex (areas AIP and VIP) and the ventral premotor cortex (areas F5 and F4). Exp. Brain Res. *128*, 181–187.

Mantini, D., Corbetta, M., Romani, G.L., Orban, G.A., and Vanduffel, W. (2013). Evolutionarily novel functional networks in the human brain? J. Neurosci. *33*, 3259–3275.

Margulies, D.S., Vincent, J.L., Kelly, C., Lohmann, G., Uddin, L.Q., Biswal, B.B., Villringer, A., Castellanos, F.X., Milham, M.P., and Petrides, M. (2009). Precuneus shares intrinsic functional architecture in humans and monkeys. Proc. Natl. Acad. Sci. USA *106*, 20069–20074.

Mars, R.B., Jbabdi, S., Sallet, J., O'Reilly, J.X., Croxson, P.L., Olivier, E., Noonan, M.P., Bergmann, C., Mitchell, A.S., Baxter, M.G., et al. (2011). Diffusion-weighted imaging tractography-based parcellation of the human parietal cortex and comparison with human and macaque resting-state functional connectivity. J. Neurosci. *31*, 4087–4100.

Mars, R.B., Sallet, J., Neubert, F.X., and Rushworth, M.F. (2013). Connectivity profiles reveal the relationship between brain areas for social cognition in human and monkey temporoparietal cortex. Proc. Natl. Acad. Sci. USA *110*, 10806–10811.

Nelissen, K., Luppino, G., Vanduffel, W., Rizzolatti, G., and Orban, G.A. (2005). Observing others: multiple action representation in the frontal lobe. Science *310*, 332–336.

Nelissen, K., Borra, E., Gerbella, M., Rozzi, S., Luppino, G., Vanduffel, W., Rizzolatti, G., and Orban, G.A. (2011). Action observation circuits in the macaque monkey cortex. J. Neurosci. *31*, 3743–3756.

Nelson, S.M., Cohen, A.L., Power, J.D., Wig, G.S., Miezin, F.M., Wheeler, M.E., Velanova, K., Donaldson, D.I., Phillips, J.S., Schlaggar, B.L., and Petersen, S.E. (2010). A parcellation scheme for human left lateral parietal cortex. Neuron *67*, 156–170.

Neubert, F.X., Mars, R.B., Buch, E.R., Olivier, E., and Rushworth, M.F. (2010). Cortical and subcortical interactions during action reprogramming and their related white matter pathways. Proc. Natl. Acad. Sci. USA *107*, 13240–13245.

O'Reilly, J.X., Beckmann, C.F., Tomassini, V., Ramnani, N., and Johansen-Berg, H. (2010). Distinct and overlapping functional zones in the cerebellum defined by resting state functional connectivity. Cereb. Cortex *20*, 953–965.

O'Reilly, J.X., Croxson, P.L., Jbabdi, S., Sallet, J., Noonan, M.P., Mars, R.B., Browning, P.G., Wilson, C.R., Mitchell, A.S., Miller, K.L., et al. (2013). Causal effect of disconnection lesions on interhemispheric functional connectivity in rhesus monkeys. Proc. Natl. Acad. Sci. USA *110*, 13982–13987.

Passingham, R.E., and Wise, S.P. (2012). The Neurobiology of the Prefrontal Cortex: Anatomy, Evolution, and the Origin of Insight. (Oxford: Oxford University Press).

Paxinos, G., Huang, X.F., and Toga, A.W. (2000). The Rhesus Monkey Brain in Stereotaxic Coordinates. (San Diego, London: Academic).

Petrides, M., and Pandya, D.N. (1999). Dorsolateral prefrontal cortex: comparative cytoarchitectonic analysis in the human and the macaque brain and corticocortical connection patterns. Eur. J. Neurosci. *11*, 1011–1036.

Petrides, M., and Pandya, D.N. (2002). Comparative cytoarchitectonic analysis of the human and the macaque ventrolateral prefrontal cortex and corticocortical connection patterns in the monkey. Eur. J. Neurosci. *16*, 291–310.

Petrides, M., and Pandya, D.N. (2007). Efferent association pathways from the rostral prefrontal cortex in the macaque monkey. J. Neurosci. *27*, 11573–11586.

Petrides, M., and Pandya, D.N. (2009). Distinct parietal and temporal pathways to the homologues of Broca's area in the monkey. PLoS Biol. *7*, e1000170.

Petrides, M., Cadoret, G., and Mackey, S. (2005). Orofacial somatomotor responses in the macaque monkey homologue of Broca's area. Nature *435*, 1235–1238.

Power, J.D., Cohen, A.L., Nelson, S.M., Wig, G.S., Barnes, K.A., Church, J.A., Vogel, A.C., Laumann, T.O., Miezin, F.M., Schlaggar, B.L., and Petersen, S.E. (2011). Functional network organization of the human brain. Neuron *72*, 665–678.

Rizzolatti, G., and Sinigaglia, C. (2010). The functional role of the parieto-frontal mirror circuit: interpretations and misinterpretations. Nat. Rev. Neurosci. *11*, 264–274.

Romanski, L.M. (2012). Integration of faces and vocalizations in ventral prefrontal cortex: implications for the evolution of audiovisual speech. Proc. Natl. Acad. Sci. USA *109* (*Suppl 1*), 10717–10724.

Rudebeck, P.H., Buckley, M.J., Walton, M.E., and Rushworth, M.F. (2006). A role for the macaque anterior cingulate gyrus in social valuation. Science *313*, 1310–1312.

Saleem, K.S., and Logothetis, N.K. (2007). A Combined MRI and Histology Atlas of the Rhesus Monkey Brain in Stereotaxic Coordinates. (London: Academic Press).

Sallet, J., Mars, R.B., Noonan, M.P., Neubert, F.X., Jbabdi, S., O'Reilly, J.X., Filippini, N., Thomas, A.G., and Rushworth, M.F. (2013). The organization of dorsal frontal cortex in humans and macaques. J. Neurosci. *33*, 12255–12274.

Scheperjans, F., Eickhoff, S.B., Hömke, L., Mohlberg, H., Hermann, K., Amunts, K., and Zilles, K. (2008). Probabilistic maps, morphometry, and variability of cytoarchitectonic areas in the human superior parietal cortex. Cereb. Cortex *18*, 2141–2157.

Schubotz, R.I., Anwander, A., Knösche, T.R., von Cramon, D.Y., and Tittgemeyer, M. (2010). Anatomical and functional parcellation of the human lateral premotor cortex. Neuroimage *50*, 396–408.

Scott, B.H., Mishkin, M., and Yin, P. (2012). Monkeys have a limited form of short-term memory in audition. Proc. Natl. Acad. Sci. USA *109*, 12237–12241.

Tomassini, V., Jbabdi, S., Klein, J.C., Behrens, T.E., Pozzilli, C., Matthews, P.M., Rushworth, M.F., and Johansen-Berg, H. (2007). Diffusion-weighted imaging tractography-based parcellation of the human lateral premotor cortex identifies dorsal and ventral subregions with anatomical and functional specializations. J. Neurosci. *27*, 10259–10269.

Verbruggen, F., Aron, A.R., Stevens, M.A., and Chambers, C.D. (2010). Theta burst stimulation dissociates attention and action updating in human inferior frontal cortex. Proc. Natl. Acad. Sci. USA *107*, 13966–13971.

Vincent, J.L., Patel, G.H., Fox, M.D., Snyder, A.Z., Baker, J.T., Van Essen, D.C., Zempel, J.M., Snyder, L.H., Corbetta, M., and Raichle, M.E. (2007). Intrinsic functional architecture in the anaesthetized monkey brain. Nature *447*, 83–86.

Wang, J., Fan, L., Zhang, Y., Liu, Y., Jiang, D., Zhang, Y., Yu, C., and Jiang, T. (2012). Tractography-based parcellation of the human left inferior parietal lobule. Neuroimage *63*, 641–652.

Yeo, B.T., Krienen, F.M., Sepulcre, J., Sabuncu, M.R., Lashkari, D., Hollinshead, M., Roffman, J.L., Smoller, J.W., Zöllei, L., Polimeni, J.R., et al. (2011). The organization of the human cerebral cortex estimated by intrinsic functional connectivity. J. Neurophysiol. *106*, 1125–1165.

Zhang, Y., Brady, M., and Smith, S. (2001). Segmentation of brain MR images through a hidden Markov random field model and the expectation-maximization algorithm. IEEE Trans. Med. Imaging *20*, 45–57.

Zhang, Y., Fan, L., Zhang, Y., Wang, J., Zhu, M., Zhang, Y., Yu, C., and Jiang, T. (2012). Connectivity-Based Parcellation of the Human Posteromedial Cortex. Cereb. Cortex. Published online November 11, 2012. http://dx.doi.org/10.1093/cercor/bhs353.